Article

Cell

Perinuclear Anchoring of H3K9-Methylated Chromatin Stabilizes Induced Cell Fate in *C. elegans* Embryos

Graphical Abstract

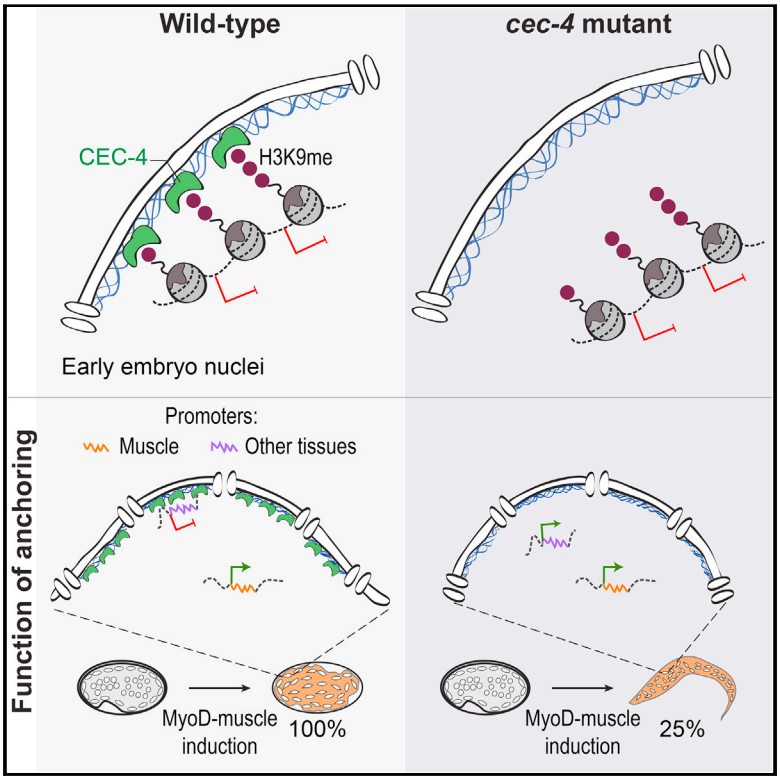

Highlights

- *C. elegans* chromodomain protein CEC-4 associates stably with the nuclear envelope
- CEC-4 anchors heterochromatin through recognition of methylated H3K9 in embryos
- Unlike loss of H3K9 methylation, *cec-4* mutant does not alter gene expression
- *cec-4* loss abrogates the embryo's ability to maintain an induced muscle cell fate

Authors

Adriana Gonzalez-Sandoval, Benjamin D. Towbin, Veronique Kalck, ..., Xinghao Wang, Kehao Zhao, Susan M. Gasser

Correspondence

susan.gasser@fmi.ch

In Brief

Selective recognition of histone H3 lysine 9 methylation by an anchor protein in the nuclear envelope enables perinuclear sequestration of chromatin in C. elegans embryos. Anchoring by CEC-4 supports full commitment to an induced muscle differentiation program.

Accession Numbers

GSE74134

Gonzalez-Sandoval et al., 2015, Cell *163*, 1333–1347
December 3, 2015 ©2015 Elsevier Inc.
http://dx.doi.org/10.1016/j.cell.2015.10.066

Cell

Perinuclear Anchoring of H3K9-Methylated Chromatin Stabilizes Induced Cell Fate in *C. elegans* Embryos

Adriana Gonzalez-Sandoval,[1,2] Benjamin D. Towbin,[1,5] Veronique Kalck,[1] Daphne S. Cabianca,[1] Dimos Gaidatzis,[1,3] Michael H. Hauer,[1,2] Liqing Geng,[4] Li Wang,[4] Teddy Yang,[4] Xinghao Wang,[4] Kehao Zhao,[4] and Susan M. Gasser[1,2,*]
[1]Friedrich Miescher Institute for Biomedical Research, Maulbeerstrasse 66, CH-4058 Basel, Switzerland
[2]Faculty of Natural Sciences, University of Basel, Klingelbergstrasse 50/70, CH-4056 Basel, Switzerland
[3]Swiss Institute of Bioinformatics, CH-4058 Basel, Switzerland
[4]China Novartis Institute of Biomedical Research Co, Ltd. Bldg 3, Lane 3728 Jinke Road, Pudong New Area, Shanghai 201203, China
[5]Present address: Department of Molecular Cell Biology, The Weizmann Institute of Science, Rehovot 76100, Israel
*Correspondence: susan.gasser@fmi.ch
http://dx.doi.org/10.1016/j.cell.2015.10.066

SUMMARY

Interphase chromatin is organized in distinct nuclear sub-compartments, reflecting its degree of compaction and transcriptional status. In *Caenorhabditis elegans* embryos, H3K9 methylation is necessary to silence and to anchor repeat-rich heterochromatin at the nuclear periphery. In a screen for perinuclear anchors of heterochromatin, we identified a previously uncharacterized *C. elegans* chromodomain protein, CEC-4. CEC-4 binds preferentially mono-, di-, or tri-methylated H3K9 and localizes at the nuclear envelope independently of H3K9 methylation and nuclear lamin. CEC-4 is necessary for endogenous heterochromatin anchoring, but not for transcriptional repression, in contrast to other known H3K9 methyl-binders in worms, which mediate gene repression but not perinuclear anchoring. When we ectopically induce a muscle differentiation program in embryos, *cec-4* mutants fail to commit fully to muscle cell fate. This suggests that perinuclear sequestration of chromatin during development helps restrict cell differentiation programs by stabilizing commitment to a specific cell fate.

INTRODUCTION

Cues stemming from the spatial organization of chromatin are widely thought to influence the function of eukaryotic genomes. Indeed, chromatin assumes distinct patterns of distribution in the interphase nucleus in response to cell-type-specific gene expression (reviewed in Meister et al., 2011; Talamas and Capelson, 2015). Dense-staining heterochromatin and repressed tissue-specific genes are sequestered at the inner nuclear membrane (INM) in both plant and animal cells. In metazoans, an INM-associated network of the intermediate filament protein lamin and other associated proteins provides a scaffold that helps the interphase nucleus reform after mitosis (Nigg, 1992).

The chromatin that associates with the nuclear lamina (lamin-associated domains or LADs) is generally gene poor, transcriptionally silent, and enriched for repressive histone marks (Gerstein et al., 2010; Guelen et al., 2008; Ikegami et al., 2010; Pickersgill et al., 2006). Importantly, in *C. elegans* embryos the integrity of two histone methyltransferases (HMTs) that target histone H3K9, MET-2, and SET-25 was shown to be essential for the peripheral localization of heterochromatin (Towbin et al., 2012). Perturbed H3K9 methylation also partially compromised proper heterochromatin organization in mammalian cells (Kind et al., 2013; Pinheiro et al., 2012). However, no nuclear envelope protein has yet been identified that anchors H3K9-methylated chromatin specifically.

Studies of nuclear organization during the development of multicellular organisms or of embryonic stem cell (ESC) differentiation in vitro showed that perinuclear chromatin sequestration is a dynamic process that changes with cell-type-specific gene expression (Fussner et al., 2010; Harr et al., 2015; Meister et al., 2010; Peric-Hupkes et al., 2010). Important genetic studies of Solovei et al. (2013) showed that heterochromatin tethering in differentiated mammalian cells depends on two partially redundant pathways that reflect the sequential induction through development of lamin B receptor (LBR) and lamin A/C. In some mouse tissues both LBR and lamin A/C are expressed; in others, expression of only one is sufficient to ensure the conventional sequestration of heterochromatin at the INM. In the absence of both perinuclear components, heterochromatin accumulated at the nuclear core (Solovei et al., 2013).

Despite these genetic implications, it was unclear what bridges chromatin to LBR or lamin A/C. LBR has been shown to bind the chromodomain (CD) of Heterochromatin proteins 1α and γ (HP1α and HP1γ; (Ye and Worman, 1996), which are hallmarks of heterochromatin. But HP1α-containing chromocenters are not necessarily perinuclear, and HP1γ is bound to many euchromatic loci positioned away from INM (Minc et al., 1999). Moreover, complete ablation of HP1α or β in either pluripotent or differentiated ESCs does not change chromocenter positioning (Mattout et al., 2015). Mammalian LBR also binds histone H4K20me2 in vitro through its C-terminal Tudor domain (Hirano et al., 2012), yet H4K20me2 is

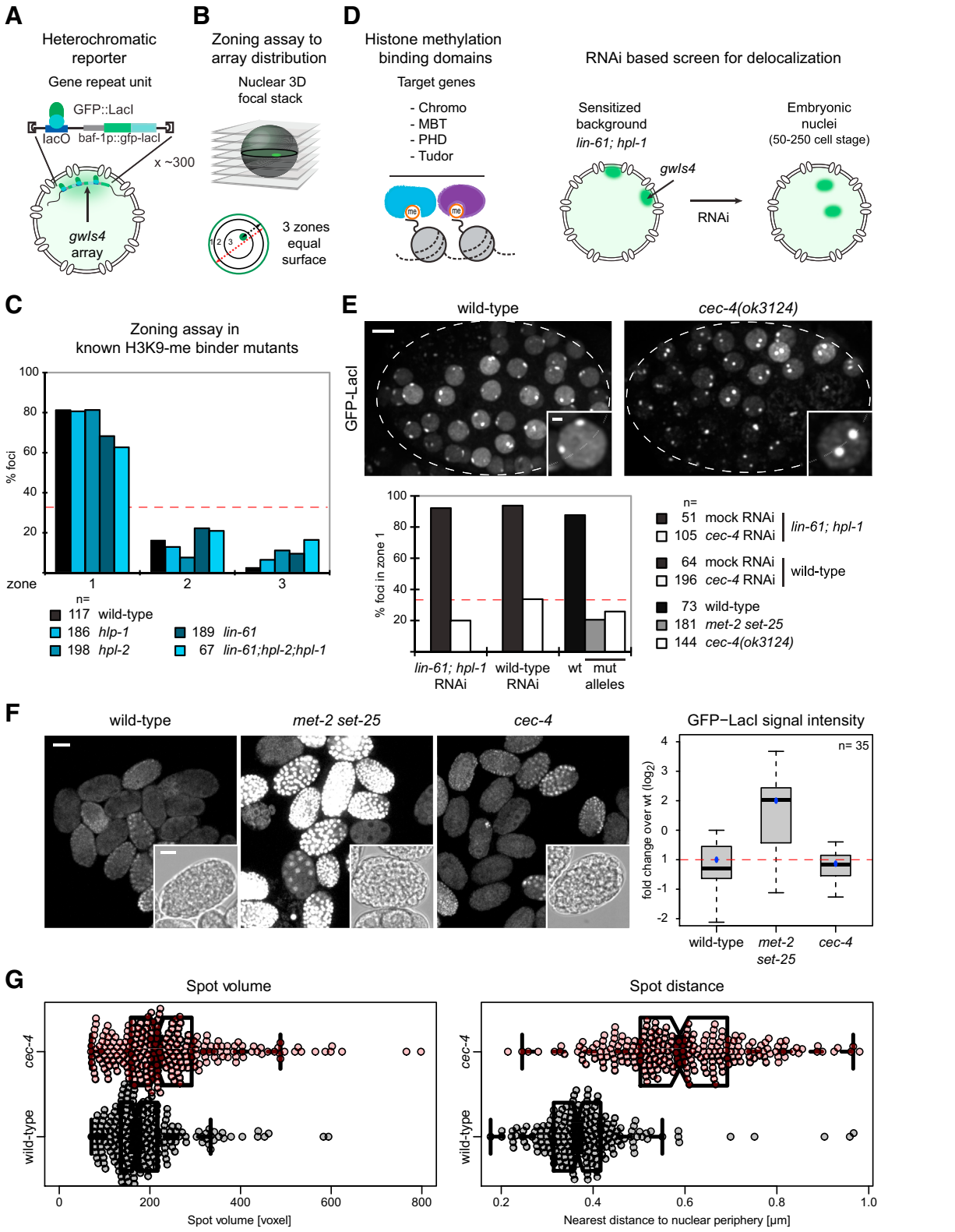

Figure 1. *cec-4* Is Required for Anchoring and Compaction of a Heterochromatic Array

(A) Heterochromatic transgene array *gwIs4 [baf-1p::GFP-lacI::let-858 3′UTR; myo-3p::RFP]* reporter.

(B) Zoning assay for array distribution. Radial position is determined relative to the INM, and values are binned into three concentric zones.

(legend continued on next page)

broadly distributed without enrichment on LADs (Barski et al., 2007).

Whereas mammalian lamins were reported to bind AT-rich DNA and histone dimers in vitro (reviewed in Wilson and Foisner, 2010), this affinity cannot account for selective heterochromatin binding. Nor is it explained by lamin A/C interaction with transcription factors or the barrier to autointegration factor (BAF), which may link specific promoters to lamins (Kubben et al., 2012; Meuleman et al., 2013). Similarly, the lamin associated Lap2β interacts with HDAC3 and the transcription factor cKrox, a ligand of GAGA motifs, leading to the repression and perinuclear anchoring of a subset of mammalian promoters (Zullo et al., 2012). Yet LADs extend far beyond promoters, coinciding instead with extensive domains of H3K9 methylation (Towbin et al., 2012).

Alternatively, nuclear lamins may act indirectly by providing a stable platform for the localization of other INM proteins (e.g., Lap2β, Emerin and Man1 [Brachner and Foisner, 2011]). Indeed, depletion of the *C. elegans* lamin, LMN-1, mislocalizes Emerin (EMR-1) and Man1 (LEM-2), and the worm Emerin in turn helps stabilize repressed muscle and neuronal genes at the INM in differentiated worm tissues (González-Aguilera et al., 2014). Yet neither Emerin nor Man1 bind heterochromatin directly. A similar indirect effect was ascribed to mammalian SAMP-1, an INM protein connected to LINC (linker of nucleo- and cytoskeleton) complex, whose loss compromises nuclear integrity and leads to Emerin, SUN-1, and Lamin A/C mislocalization (Gudise et al., 2011). Finally, loss of PRR14, a perinuclear HP1-binding protein, altered perinuclear attachment of H3K9-methylated domains in mammalian nuclei, yet led to general defects in nuclear structure, raising the question of indirect effect on DNA localization (Poleshko et al., 2013).

Here we exploit the power of RNAi screens in the nematode *C. elegans* to find a methyl-H3K9-specific perinuclear anchor for heterochromatin. We have individually downregulated genes that harbor characteristic histone methylation binding motifs and monitored changes in the perinuclear anchoring of heterochromatin in early embryos. We identified a previously uncharacterized *C. elegans* CD protein, CEC-4, as our only positive hit. CEC-4 localizes at the INM where it directly binds endogenous H3K9-methylated chromatin through its CD's aromatic cage. CEC-4 is not necessary for the transcriptional silencing of either endogenous genes or a heterochromatic reporter, although the methylation of H3K9 and its ligands HPL-2 and LIN-61 are. Despite this, a reproducible fraction of *cec-4* embryos were unable to maintain the muscle specification induced by a pulse of HLH-1 (MyoD) expression. We suggest that perinuclear sequestration of chromatin contributes to cell fate commitment under conditions of perturbed development.

RESULTS

CEC-4 Is a Chromodomain Factor that Anchors a Heterochromatic Array

To search for proteins involved in the anchoring of methylated H3K9 chromatin, we designed an RNAi screen with a fluorescent reporter for perinuclear heterochromatin positioning in *C. elegans* embryos. Our reporter is an integrated plasmid array, *gwIs4*, which expresses the GFP-LacI fusion protein under control of the ubiquitously active *baf-1* promoter. GFP-LacI binds a *lacO* site that occurs once per 3.5 kb (~300x), generating a fluorescent focus that binds the INM in embryonic nuclei (Figure 1A). The histones on the array are trimethylated on H3K9 and H3K27, but lack H3K4 methylation, and have reduced gene expression, thereby recapitulating conserved features of heterochromatin (Meister et al., 2010; Towbin et al., 2010). Array position is determined with a zoning assay in which radial distances from the spot to the nuclear periphery, scored in the focal plane in which the spot is the brightest, are binned into 3 zones of equal surface (Figure 1B). Deviation from 33% indicates nonrandom localization.

The *C. elegans* genome encodes 65 proteins that contain methyl-lysine/-arginine binding motifs, namely CD, MBT (malignant brain tumor), PHD (plant homeodomain) and Tudor domains (Table S1; reviewed in Taverna et al., 2007). This set of proteins includes HPL-1 and HPL-2, homologs of HP1, a highly conserved CD protein that binds methylated H3K9 to silence heterochromatin (Nestorov et al., 2013). HPL-1 co-localizes with the heterochromatic *gwIs4* array in worm embryos and appears to repress transcription in a promoter-specific manner working together with the H1 variant HIS-24 in larvae (Studencka et al., 2012a). HPL-2 binds H3K9me2/3 as well as H3K27me2/3 in vitro, and it is needed to repress large heterochromatic arrays in both embryos and germline cells, as well as to fine-tune other gene expression events (Couteau et al., 2002; Studencka et al., 2012b). A third H3K9me2/me3 ligand is the MBT-domain protein LIN-61, whose loss compromises vulva development, silencing of heterochromatic arrays, and a neuron-specific reporter in somatic cells (Koester-Eiserfunke and Fischle, 2011; Zheng et al., 2013). Remarkably, elimination of these known H3K9me ligands,

(C) Array distribution quantitation, as described in (B), in early embryos (50–250 cell stage) of indicated genotypes (Tables S1 and S3). Red line = random distribution of 33%.

(D) Design of candidate RNAi screen in *lin-61;hpl-1* deficient strain. L1 larvae subjected to RNAi for candidates listed in Table S3, and embryonic progeny screened for array delocalization.

(E) Z-projection of representative embryos bearing *gwIs4* in WT and *cec-4(ok3124)* strains. Insets: single nuclei. Scale bar, 5 or 2 μm, respectively. Array distribution, zone 1 data in early embryos as indicated, n = foci scored per condition. Pair-wise comparisons of mock RNAi and WT conditions with *cec-4* RNAi or mutant yielded p values < 0.001 by χ^2 test.

(F) Z-projection of GFP fluorescence in embryos of indicated genotype with *gwIs4*. Insets: bright field. Scale bar, 20 or 10 μm, respectively. Quantified signal intensity displayed as box plot in $\log_2$ scale, whiskers = 1st and 3rd quartiles. Black lines: median, blue dots: mean, red dashed line: baseline = mean of WT. n = embryos scored.

(G) 3D spot volume and distance from INM in WT and *cec-4(ok3124)* embryos. Notched box plots overlapping individual measurements as above. n = 209 and 237, respectively, from five embryos each; pair-wise comparisons with p-values < 0.001 by Student's t test.

See also Figure S1.

singly or in combination, had little impact on the perinuclear sequestration of the *gwIs4* heterochromatic array, although the mutants did lose transcriptional repression (Figure 1C; Towbin et al., 2012).

Conscious that anchor redundancy might be a concern, we downregulated other methyl-binding candidates by RNAi in *hpl-1;lin-61* double mutant embryos. Only one RNAi target, *cec-4,* which encodes an uncharacterized CD protein, affected the perinuclear anchoring of the heterochromatic reporter (Figures 1D and 1E). The percentage of heterochromatic foci in the outermost nuclear zone dropped from 92% to 20%, following *cec-4* RNAi (Figures 1E and S1B). Although *cec-3/eap-1* has been described as an H3K9me1-3 binder involved in neuron-specific gene expression (Greer et al., 2014; Zheng et al., 2013), *cec-3* RNAi had no impact on heterochromatin anchoring in our screen (data not shown).

The effect of *cec-4* RNAi on array position did not depend on the absence of LIN-61 or HPL-1, for the same RNAi in WT worms yielded identical array delocalization (Figures 1E and S1B). To rule out off-target effects of *cec-4* RNAi, we scored array position in embryos carrying the null mutant *cec-4(ok3124),* which lacks the 5′ UTR and first 2 exons (Figure S1A). The genetic ablation of *cec-4* phenocopied *cec-4* RNAi, yielding full array detachment from the INM, identical to that scored in embryos that lack H3K9 methylation; i.e., the *met-2 set-25* double mutant (Towbin et al., 2012). Thus, the CD-encoding *cec-4* gene is required, like H3K9-methylation, for the perinuclear anchoring of heterochromatic arrays in *C. elegans* early embryos.

We examined the effect of *cec-4* ablation on gene expression by quantifying the fluorescent intensity of GFP-LacI, which is expressed from a housekeeping promoter on the *gwIs4* array. Although the expression levels are strongly upregulated in *met-2 set-25* mutant, deletion of *cec-4* did not alter GFP-LacI expression in embryos (Figure 1F). Both H3K9me3 and the enzyme mediating this terminal modification, SET-25, remained enriched on the delocalized array in *cec-4* mutant embryos (Figures S1C and S1D), consistent with the observed transcriptional repression. We conclude that CEC-4-mediated anchoring is not essential for heterochromatic array repression. Nonetheless, coupled with the loss of anchoring we scored a significant decompaction of the reporter, upon release from the INM. Monitored by a quantitative 3D volume rendering protocol, we found that the mean volume expanded from about 192 to 239 voxels upon *cec-4* deletion (Figure 1G).

CEC-4 Localizes Intrinsically to the Nuclear Periphery

We next examined the subcellular localization of CEC-4. A mCherry-tagged version of *cec-4* was integrated as a site-specific, single-copy genomic insertion under control of its endogenous *cec-4* promoter and 3′UTR (Figure S2A). Confocal fluorescence microscopy of CEC-4-mCherry (CEC-4-mCh) showed that the protein forms a ring at the nuclear periphery at all embryonic stages (Figure 2A). This distribution persisted in larval and adult differentiated tissues and in the germline of adult worms (Figure 2D; data not shown). CEC-4 localization was independent of H3K9 methylation; the same perinuclear CEC-4-mCh ring was found in the *met-2 set-25* mutant, in which H3K9 is unmethylated and heterochromatin was delocalized and expressed (Figure 2C). Only in mitosis did CEC-4-mCh become dispersed (data not shown), much like lamins, which undergo phosphorylation by cyclinB/Cdk in mitosis (Nigg, 1992).

Quantification of fluorescence intensity of CEC-4-mCh in L1 larval stage showed protein level variation in a tissue-specific fashion. CEC-4 is weakly expressed in intestine, highly expressed in muscle, and is found at intermediate levels in almost every other tissue (Figure 2D). This unequal tissue-specific expression was not observed for an EMR-1 fusion construct designed and integrated in a similar manner (EMR-1-mCherry; Figures 2D and S2A).

To characterize CEC-4's nuclear rim pattern further, we imaged embryos at 100 nm resolution using super-resolution structured illumination microscopy (SR-SIM). The CEC-4-mCh ring resolved into a perinuclear, punctate pattern (Figure 2B), and counterlabeling of nuclear pores or LMN-1 (lamin) showed CEC-4 in the same concentric plane as lamin and is situated mostly between pores (Figure 2B). Lamin and CEC-4-mCh were in very close proximity, yet could be resolved as distinct foci (low yellow signal in red/green channel merge; Figure 2B), suggesting that CEC-4 might localize to the INM independently of lamin. Indeed, after treating these worms with *lmn-1* RNAi, CEC-4 perinuclear ring persisted (data not shown). The same was true after RNAi against Emerin, LEM-2, SUN-1, UNC-84, BAF-1, and all other known *C. elegans* INM components (Table S6).

We reasoned that if CEC-4 localizes independently of lamin, it might also associate with the nuclear envelope of budding yeast, which lacks lamin entirely (reviewed in Taddei and Gasser, 2012). Indeed, when expressed as a GFP fusion protein under control of the *GAL1* promoter, CEC-4-GFP formed a perinuclear ring at INM of yeast nuclei (Figure S2B). To map the domain that directs CEC-4 to the INM, we expressed complementary N- and C-terminal fragments of CEC-4, fused to GFP. Both yielded a diffuse nuclear distribution (Figure S2C), suggesting that the integrity of the holoprotein is necessary for INM enrichment (Figure S2C). Similar results were obtained with similar constructs expressed ectopically in *C. elegans* (data not shown). Finally, in yeast as in worms, ablation of known INM and pore basket proteins (Table S7) did not alter CEC-4-GFP localization. We therefore propose that either CEC-4 has an intrinsic affinity for the INM, or else it binds a conserved but uncharacterized membrane component.

CEC-4 Chromodomain Preferentially Binds Methylated H3K9

Based on sequence analysis, the CEC-4 CD (aa 82–141) shares 42% identity with mammalian HP1α CD and 33% with HPL-1/2 CDs, yet CEC-4 lacks the HP1-specific chromoshadow and RNA-binding hinge domains (Couteau et al., 2002). Protein comparison failed to reveal a strict homolog of CEC-4 in mammalian genomes, apart from the CD and a second conserved motif, here called PD (putative domain, aa 25–76), which is found in other CD-containing proteins (Figure 3A).

The CEC-4 CD has a canonical secondary structure like mammalian HP1 and Pc3 (Fischle et al., 2003b), with an aromatic cage containing two tyrosine residues that are predicted to recognize methylated lysine within the H3 ARK(S/T) motif. To characterize the specificity of CEC-4 CD binding, we expressed

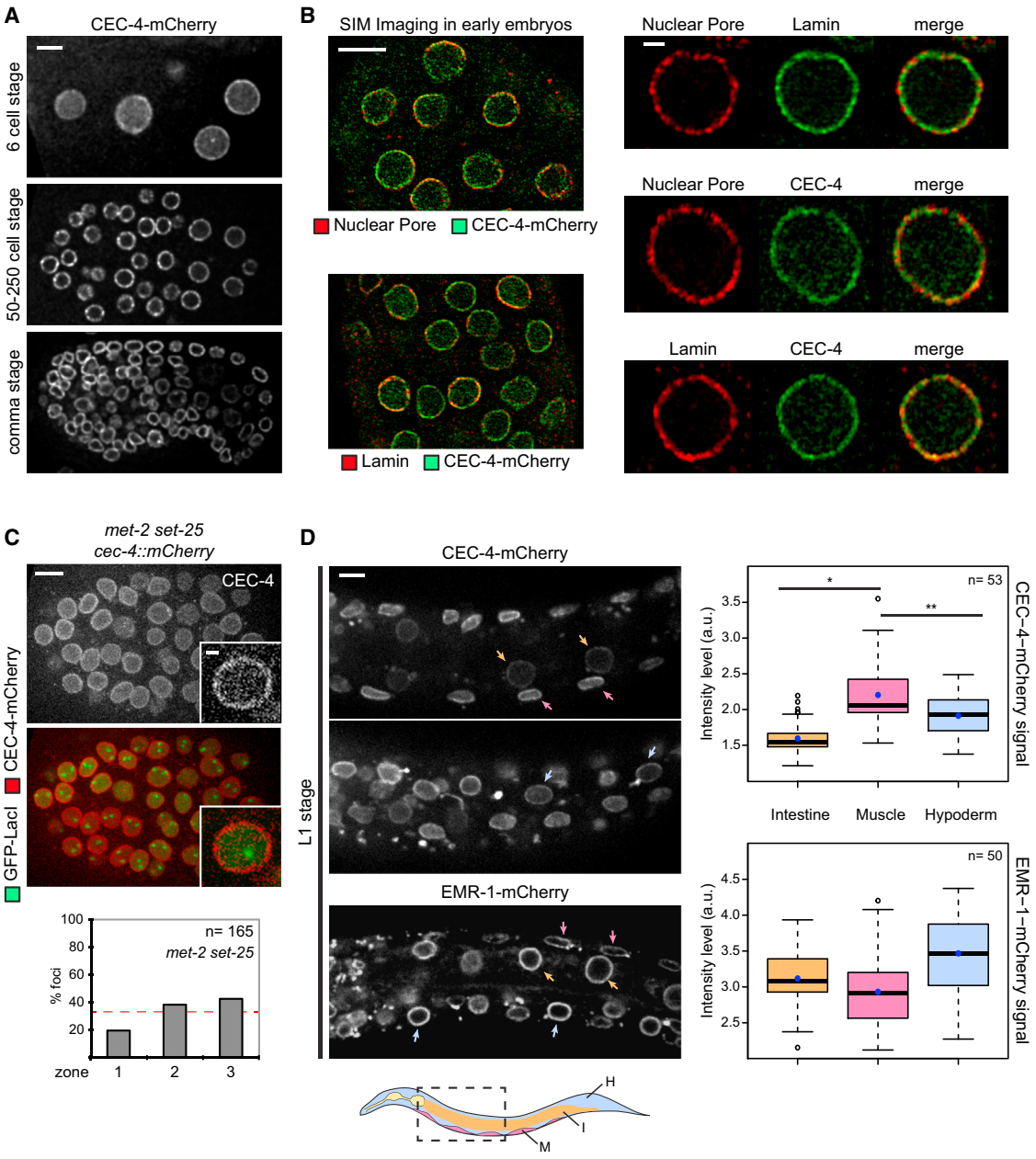

Figure 2. Perinuclear CEC-4 Localization Is Independent of H3K9 Methylation, and Varies from Tissue to Tissue

(A) Single plane images of indicated embryo stages expressing CEC-4-mCh.

(B) SR-SIM microscopy of CEC-4-mCh transgenic embryos, counterstained for nuclear pores, lamin or mCherry. Embryo sections and single nuclear planes shown.

(C) Z-projection of CEC-4-mCh in *met-2 set-25* mutant background; images of mCherry alone and merged with *gwIs4* GFP-LacI signal are shown. Insets: single plain nuclei. Quantification of array distribution, n = foci scored.

(D) Single plane confocal images of CEC-4- and EMR-1-mCh transgenic L1 larvae; scheme of L1 worm color-coded by tissue, M: muscle, I: intestine, H: hypoderm. Measured mCh signal intensity displayed as box plots in a.u. as in Figure 1. Black circles = outliers, n = number of nuclei per tissue; pair-wise comparisons for * and **p value < 0.001 in Wilcoxon test. Scale bar, 5 μm in whole/section embryos and larvae; 2μm in single nuclei/insets.

See also Figure S2.

and purified the WT CD-containing fragment of CEC-4 (CEC-4 CD; aa 25–141) and a mutated version of the same fragment (Y87A and Y111A; CEC-4 cd-2YA; Figures 3A and S3A), bearing point mutations that should disrupt the aromatic cage. Using magnetic beads coated with unmethylated (me0) or tri-methylated (me3) H3K9 peptide (aa 1–20+Cys), we found that the WT CEC-4 CD bound a H3K9me3 peptide specifically, while the CEC-4 cd-2YA mutant fragment did not (Figure 3B).

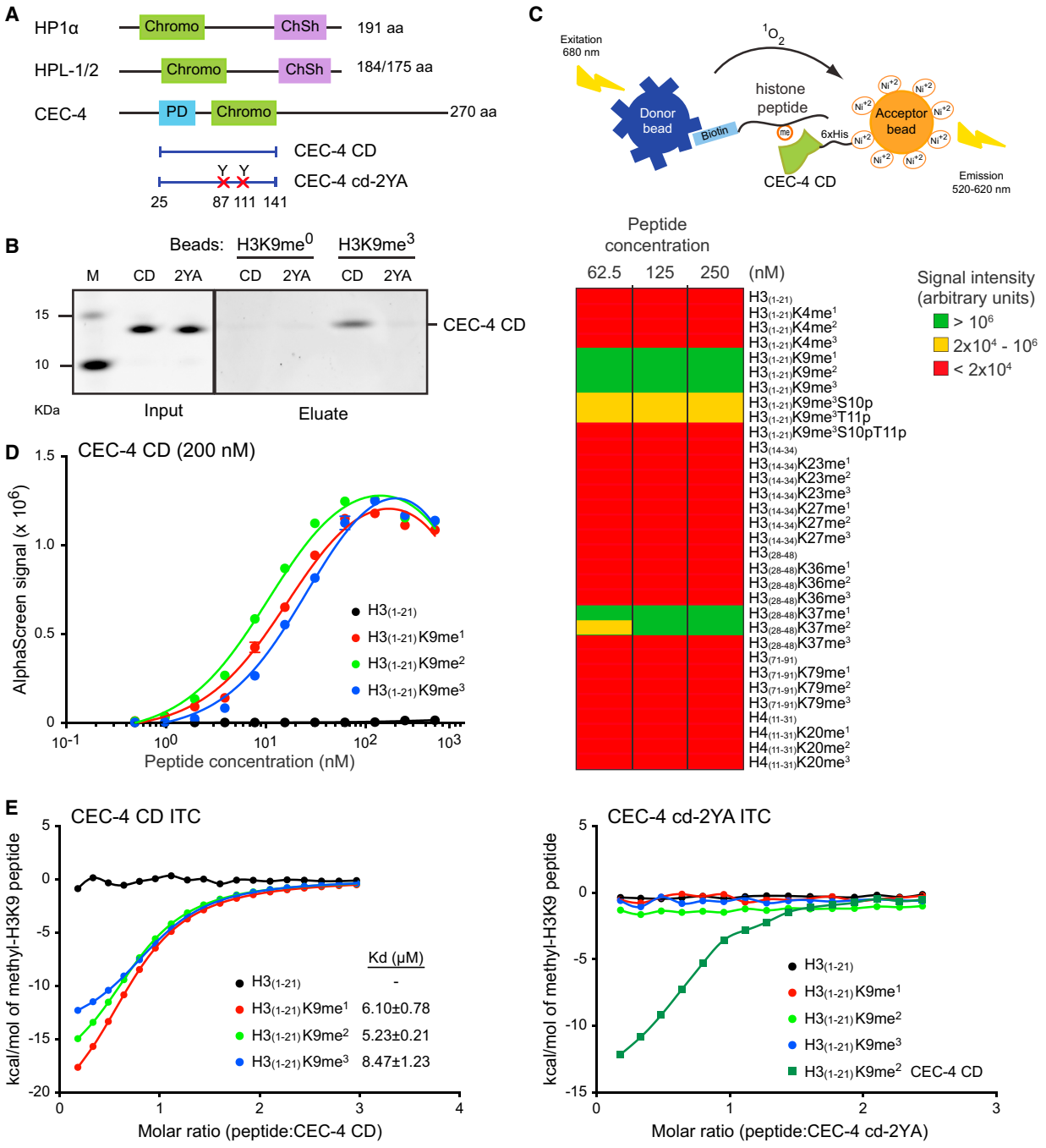

Figure 3. CEC-4 CD Binds Methylated H3K9 Peptides

(A) Schematic comparison of *H. sapiens* HP1α, *C. elegans* HPL-1/2 and CEC-4. CD (green), purple: chromoshadow (ChSh) domain, blue: conserved PD. Purified CEC-4 CD fragments in blue; red X = Y87A and Y111A mutations.

(B) Pull-down of recombinant His-tagged CEC-4 CD fragments (A) by unmodified or me3-H3K9 resin-immobilized peptides. Protein visualized by SYPRO Ruby staining.

(C) AlphaScreen scheme: donor and acceptor microbeads coated with 188 different biotinylated peptides and His-tagged CEC-4 CD, respectively. Interaction produces a fluorescent signal through singlet oxygen ($^1O_2$) transfer from donor to Ni^{+2} ions on acceptor beads. Three peptide concentrations tested with equal amounts of CEC-4 CD (200 nM). Color-coded results reflect signal intensity (see Table S4 for rest of library).

(D) Dose-response binding curves for indicated H3K9 peptides with CEC-4 CD in AlphaScreen assay.

(E) Quantitation of binding affinities of H3K9 peptides to CEC-4 CD and cd-2YA mutant determined by ITC. In (D) and (E) solid lines represent a nonlinear least-square fit using one-sided fitting equation.

See also Figures S3 and S4.

We evaluated CEC-4 CD specificity by scoring interaction with a range of modified and unmodified histone tail peptides in a quantitative chemiluminiscence assay (Alpha Screen; Taouji et al., 2009). We screened the ALTA Biosciences library, which contains 188 histone tail ligands each with a different epigenetic modification (Table S4; Figure 3C). Consistent with the pull-down assay, strong interaction signals were detected almost exclusively between CEC-4 CD and a peptide of histone H3 bearing me1-, me2-, or me3-K9. Intriguingly, CEC-4 affinity for H3K9me3-containing peptides was compromised by additionally phosphorylating S10 and/or T11 (Figure 3C and Table S4). Such modifications have been proposed to release HP1 from chromatin in mitosis (Fischle et al., 2003a).

The interaction of CEC-4 CD with methylated H3K9 was confirmed by serial dilutions of each peptide in the AlphaScreen (Figure 3D) and IC_{50} (half maximal inhibitory concentration) was determined by peptide displacement. CEC-4 CD bound to me1-, me-2, or me3-K9 H3 peptides with similar affinities (Figure S3C). We then measured binding energies using Isothermal Titration Calorimetry (ITC). Dissociation constants (Kd) for CEC-4 CD bound to the methylated H3K9 peptides ranged from 5 to 9 μM. There was a slight preference for me2 and no detectable binding to the unmodified H3 peptide (Figures 3E, S3D, and S4A). Similar Kd values have been reported for human, mouse, and *Drosophila* HP1 homologs (reviewed in Steffen et al., 2012). The interaction requires the characteristic aromatic cage of the CEC-4 CD, as CEC-4 cd-2YA gave only background level interaction (Figures 3E and S4A). We conclude that CEC-4 CD recognizes H3K9me1, me2, and me3. Its affinity for all three methyl-H3K9 forms is consistent with the fact that heterochromatic arrays remain peripherally sequestered in the *set-25* mutant, which has H3K9me1/me2, but no H3K9me3 (Towbin et al., 2012).

In addition to its strong affinity to H3K9me-peptides, we detected interaction of the CEC-4 CD with me1- or me-2 H3K37 (aa 28–48; Figures 3C and S3B; Table S4). Methylation of H3K37 has not been reported to occur in native *C. elegans* chromatin and was not detected in our own mass spectrometry of embryonic histones (data not shown; Towbin et al., 2012). To date, the only documented occurrence of H3K37me1 is in tandem with H3K36me1 at origins of replication in budding yeast, outside of S phase (Unnikrishnan et al., 2010). However, CEC-4 did not recognize H3K36me. In addition, CEC-4 CD had significantly lower affinity for H3K37me than for methylated H3K9 (Figures S3D, S3E, and S4B). Thus, the physiological relevance of this second binding site is unclear.

The CEC-4 CD Is Essential for Heterochromatin Anchoring in Embryos, but Is Redundant in Differentiated Tissues

The single-copy CEC-4-mCh fully restores array anchoring in the *cec-4* null mutant. It is enriched on the anchored heterochromatic reporter due to its affinity for H3K9me (Figures 4A and S2C). An identical integration construct bearing the aromatic cage mutations described above (CEC-4cd-2YA-mCh) did not complement for anchoring, nor did it bind to the array (Figure 4B). Thus, disruption of the CEC-4 CD aromatic cage is sufficient to disrupt the anchoring of heterochromatin at the INM in embryos and the binding of methylated H3K9 peptides in vitro. On the other hand, CD integrity is not involved in CEC-4 localization, given that CEC-4cd-2YA-mCh forms a perinuclear ring like WT CEC-4-mCh (Figure 4B).

In contrast to the situation in embryos, the ablation of *cec-4* did not provoke relocalization of the heterochromatic array in differentiated L1 larval tissues, such as intestine and hypoderm (Figure 4C). The same was observed in the *met-2 set-25* double mutant (Towbin et al., 2012). It appears, therefore, that compensatory or redundant mechanisms for anchoring heterochromatin are induced in the differentiated tissues of the L1 larva. It is unclear whether these mechanisms are fully independent of CEC-4 or if CEC-4 contributes to tissue-specific anchoring in a redundant manner (Figure 2D). Both the redundancy and tissue-specificity aspects are reminiscent of lamin A/C and LBR effects in mice (Solovei et al., 2013).

Loss of CEC-4 Alters the Spatial Distribution of Endogenous Chromosome Arms

Thus far integrated transgenic arrays were used as a surrogate for heterochromatin. To see if CEC-4 affects the distribution of endogenous chromatin, we performed LEM-2 chromatin immunoprecipitation coupled to deep sequencing (ChIP-seq) in WT and mutant embryos. *C. elegans* chromosomes are holocentric and lack pericentric satellite heterochromatin but are enriched for H3K9 methylation and repetitive elements along the distal arms of all autosomes and the left arm of chromosome X(Gerstein et al., 2010; Ikegami et al., 2010). Previous ChIP and lamin-Dam-ID studies had shown that chromosome arms are proximal to the INM in *C. elegans* embryos, larvae, and adults. Moreover, the loss of H3K9 methylation (*met-2 set-25*) was enough to compromise INM-anchoring of the repeat-rich autosomal arms (González-Aguilera et al., 2014; Ikegami et al., 2010; Towbin et al., 2012).

We used ChIP-seq to map LEM-2-binding along endogenous sequences in WT, *cec-4*, and *met-2 set-25* embryos. Euclidian distances were measured showing high similarity between replicas. Hierarchical clustering resolved WT LEM-2 ChIP as different from either mutant, while the *met-2 set-25* and *cec-4* mutants clustered together (Figure S5A). All input samples were very similar. Plotting the LEM-2 signals along the chromosomal sequences showed that distal arms lost anchoring in *cec-4* null embryos to the same degree as in the H3K9me-deficient *met-2 set-25* mutant (Figures 5A and S5B).

As expected, LEM-2 binding along wild-type autosomes was polarized: chromosome arms were enriched at the INM and centers were depleted. This polarization was reduced for each autosome similarly in both mutants. The integrated LEM-2 signal on each chromosomal extremity was plotted against the signal integrated over each center, to visualize the effects of the mutations (Figure 5B). We conclude that the INM binding of the endogenous repeat-rich domains on chromosome arms requires H3K9 methylation and its recognition by CEC-4. Nonetheless, other positioning pathways likely exist, since chromosome extremities were displaced to different degrees.

In many organisms heterochromatin is also clustered around the nucleolus, the site of rDNA transcription by RNA Pol I (Padeken and Heun, 2014). The *C. elegans* rDNA is found on the

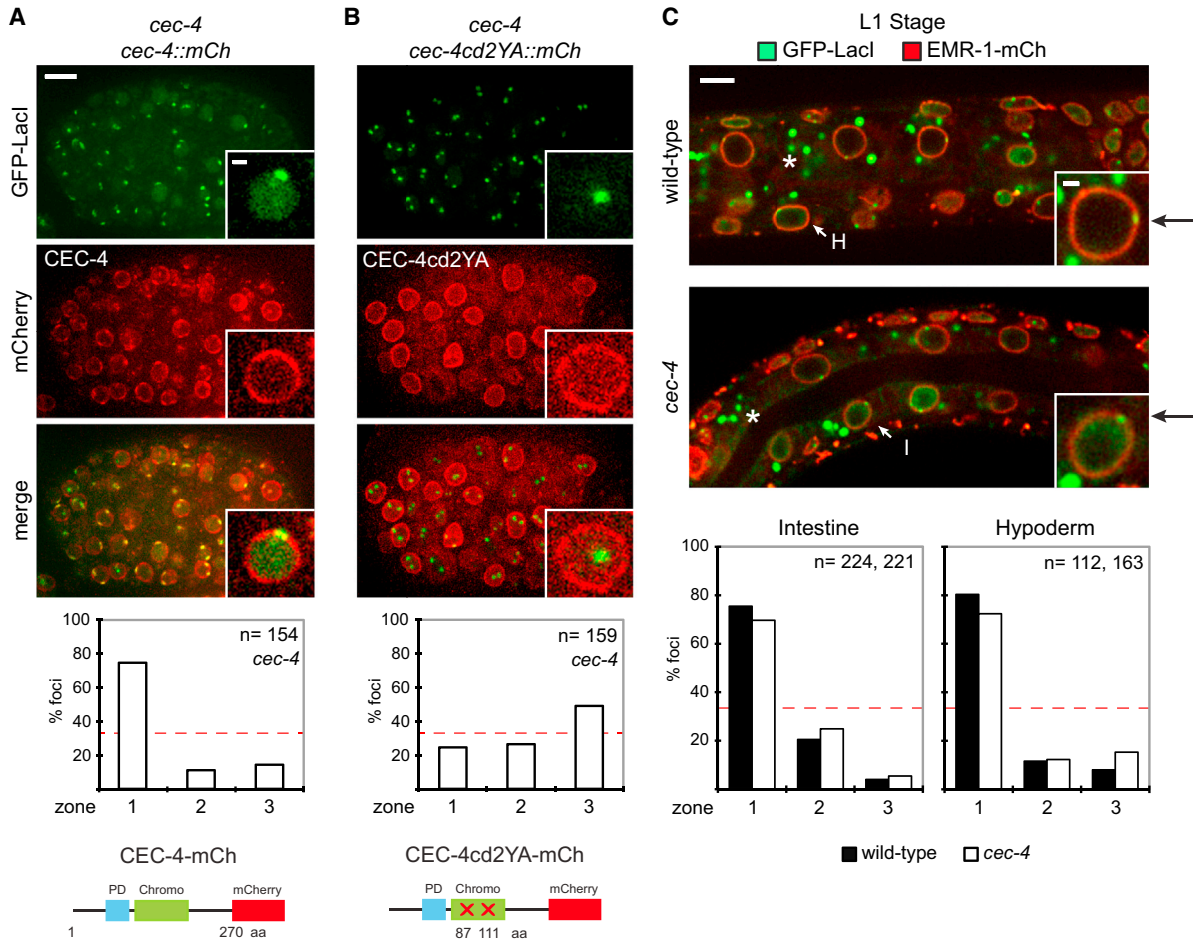

Figure 4. CEC-4 CD-H3K9me Recognition Required for Heterochromatic Array Anchoring in Embryos, while Larvae Have Compensatory Pathway(s)

(A) Z-projections showing co-localization of *gwIs4* GFP-LacI signal with CEC-4-mCh in *cec-4* null embryos. Insets: single nucleus. Zoning assay for array distribution, n = foci scored. Schematic view of transgenic protein expressed.

(B) Same as (A), except that CEC-4 transgene contains CD mutations (CEC-4cd2YA-mCh). Pair-wise comparison of (A) and (B) graphs with p value < 0.001, χ^2 test.

(C) Single plane images of L1 stage worms containing *gwIs4* and EMR-1-mCh in indicated genotypes. White arrows indicate hypoderm (H) or intestine (I) cells; * marks granule intestine foci. Insets: intestine nuclei, black arrows = array foci. Zoning assay on indicated tissues, n = foci scored per condition. Scale bars, 5 μm in embryos/L1 sections and 2 μm in single nuclei.

See also Figure S2.

distal arms of ChrI and ChrV in heterochromatic regions (Figure 5A). We therefore checked whether nucleoli change their radial position in the *cec-4* mutant by staining for a conserved marker of the nucleolus, fibrillarin (Figure 5A). In embryos lacking CEC-4, nucleoli shifted quantitatively away from the perinuclear lamin (Figure 5C), confirming that CEC-4 contributes profoundly to the positioning of endogenous chromatin in embryos.

Monitoring Gene Expression in the Absence of CEC-4

It has long been debated whether nuclear localization is sufficient to influence gene expression. To test this we generated gene expression profiles (RNA-seq) of WT, *met-2 set-25*, and *cec-4* mutant embryos. Pairwise comparison of two independent biological replicas of mutant and WT samples showed a reproducible upregulation (>4-fold) of a large number of genes in embryos lacking H3K9 methylation (*met-2 set-25)*, whereas the loss of CEC-4 led to robust upregulation of a single gene, *srw-85* (Figure 5D). The modest effect of *cec-4* mutation on gene expression is consistent with our results from the array-borne GFP-LacI (Figure 1F). In the case of endogenous genes in early embryos, the lack of derepression might simply reflect the absence of transcription factors needed for tissue-specific gene expression. However, given that the loss of H3K9 methylation does upregulate many genes in embryos, it is more likely that H3K9me-ligands other than CEC-4 mediate gene repression. Analysis of datasets in 500 bp windows across the whole genome, for potential changes in non-genic regions, yielded similar results to the gene-centric analysis; only genomic

windows spanning the *srw-85* locus were reproducibly upregulated in *cec-4(ok3124)* (Figure S5C).

The dramatic induction of *srw-85* (> 16-fold) upon displacement from the INM is a notable exception (Figures 5A and 5D–5F). Its derepression correlates strongly with subnuclear position, and not with H3K9 methylation state, as it was not derepressed in *met-2* or *set-25* single mutant embryos, which retain anchoring (Towbin et al., 2012). SRW-85 is a member of the *C. elegans* chemoreceptor family of seven transmembrane G protein-coupled receptors (7TM-GPCR). The gene sits on ChrV-right, along with 90% of the 145 *srw* family members, and is normally expressed in non-ASE type (gustatory) neurons (Etchberger et al., 2007). Given that surrounding genes are not equally upregulated (Figure S5D), we conclude that *srw-85* is an exception rather than the rule. CEC-4, unlike other H3K9 methylation readers, serves primarily to position chromatin, although the H3K9me2/me3 modification it recognizes also mediates transcriptional silencing.

Perinuclear Anchoring Helps Stabilize an Ectopically Induced Cell Differentiation Program

We examined *cec-4* mutant worms for developmental defects. Surprisingly, we found no drop in brood size nor embryonic lethality (either at 20°C or 26°C). We scored no reproducible differences in the developmental timing of embryonic stages, and except for a slight increase in the proportion of male progeny, proliferation appeared normal under standard laboratory conditions (data not shown). Given that alternative anchoring pathways are induced in L1 larvae, we sought to test the role of CEC-4-mediated chromatin tethering specifically in embryos.

To this end, we used an assay that induces muscle cell specification in embryos in response to a cell-type independent burst of HLH-1 (MyoD) expression, a master regulator for muscle differentiation (Fukushige and Krause, 2005). Induction of HLH-1 is driven by the *hsp-16.2* heat-shock (HS) promoter on a transgene array (*HS::hlh-1*) and is achieved by placing embryos at 34°C for 10 min; about 24 hr after, efficiency of induction can be monitored by morphology and muscle-specific gene expression (Figure 6A). To test whether *cec-4* mutant alters the efficiency of muscle induction, we introduced the *HS::hlh-1* transgene and the *gwIs4* array into WT and *cec-4* mutant, using the latter as a fluorescent reporter for muscle-specific gene expression (*myo-3p::RFP*). At 40 min after HS, *hlh-1* mRNA was expressed at comparable levels in both genotypes, as was the downstream muscle specific myosin, *myo*-3, at 24 hr after HS (Figure 6B).

We induced HLH-1 expression at different time points during synchronized embryonic growth and monitored the outcome by microscopy. A striking difference between WT and mutant embryos was noted when we exposed the bean stage (~560 cells; 300 min growth at 22.5°C) to the HLH-1 pulse (Figure 6C–6F). Whereas 100% of the wild-type embryos turned into lumps of muscle-like cells with muscle-twitching behavior, among the heat-shocked *cec-4* null embryos a reproducible 25% continued to develop, reaching the point of hatching from the eggshell despite their documented HLH-1 expression (Figure 6C and 6D). These hatched larva-like organisms were clearly abnormal, as they were disrupted by the slightest manipulation and failed to survive. Nonetheless, they had progressed well beyond embryonic stages and did not manifest the muscle morphology of their WT counterparts (Figure 6C and 6E). To rule out a general temperature sensitivity of *cec-4* deletion, we exposed the mutant embryos lacking the *HS::hlh-1* to HS, yet observed no effect on development: all embryos yielded normal larvae (Figure 6C).

After HLH-1 induction, the fluorescent reporter *myo-3p::RFP* was detected in patches of cells in both genotypes, with an overall higher intensity in WT cells (Figures 6E and S6A). The subset of *cec-4* mutant embryos that became muscle, like the WT embryos, showed twitching behavior. In contrast, the *cec-4* null hatched larva-like worms had a dispersed *myo-3p::RFP* expression pattern throughout the organism, which was distinct from the usual *myo-3* expression pattern in L1 larvae body wall muscle (Figure 6E). We could complement the *cec-4* deletion by introducing the tagged CEC-4-mCh; indeed, this restored the normal WT response to HLH-1 induction, and 100% of the embryos became muscle cells. In contrast, complementing with CEC-4cd2YA-mCh yielded results reminiscent of the *cec-4* null, albeit less penetrant (Figure S6B).

The inefficiency of the *cec-4* mutant for muscle tissue conversion in response to MyoD, appears to reflect an inability to lock in the muscle specification program and repress other differentiation programs. In other words, despite high level expression of HLH-1, the *cec-4* mutant appeared to remain more permissive to other differentiation signals and therefore continued to develop other tissues while expressing muscle-specific genes. We confirmed this by tracking an intestine cell marker that is not expressed in either genotype at the bean stage when we perform HS. The reporter (kind gift of G.-J. Hendriks and H. Grosshans, personal communication) expresses a GFP-tagged nuclear pore protein from an L1-stage gut-specific promoter (*nhx-2*). At 18 hr after HS, we find that the fluorescent gut marker (*nhx-2p::npp-9::GFP*) was detected in 94.5% of *cec-4* mutant embryos, but significantly less in WT (39.6%; Figure 6F).

Given the fragility of the hatched larvae-like structures, neither immunostaining nor manual isolation for RNA-seq was possible. However, their morphology alone allows one to conclude that a significant fraction of the *cec-4* mutant embryos failed to restrict gene expression to the muscle program. Thus, the perinuclear sequestration of silent genes by CEC-4 in embryonic stages appears to help stabilize the HLH-1-induced muscle cell fate.

DISCUSSION

Perinuclear Chromatin Sequestration through Histone H3K9 Methylation

Heterochromatin, or transcriptionally silenced chromatin, is often juxtaposed to the INM in eukaryotic organisms. Previous work has identified H3K9 methylation as essential for heterochromatin anchoring in worms (Towbin et al., 2012) and important in mammalian cells (Kind et al., 2013; Pinheiro et al., 2012). However, no INM anchor that selectively binds this epigenetic mark was known. Here we describe CEC-4 as a perinuclear *C. elegans* protein which is necessary for the tethering of endogenous chromatin bearing me1-, me2-, or me3-H3K9 histones. Its CD's aromatic cage is necessary for H3K9me binding in vitro and

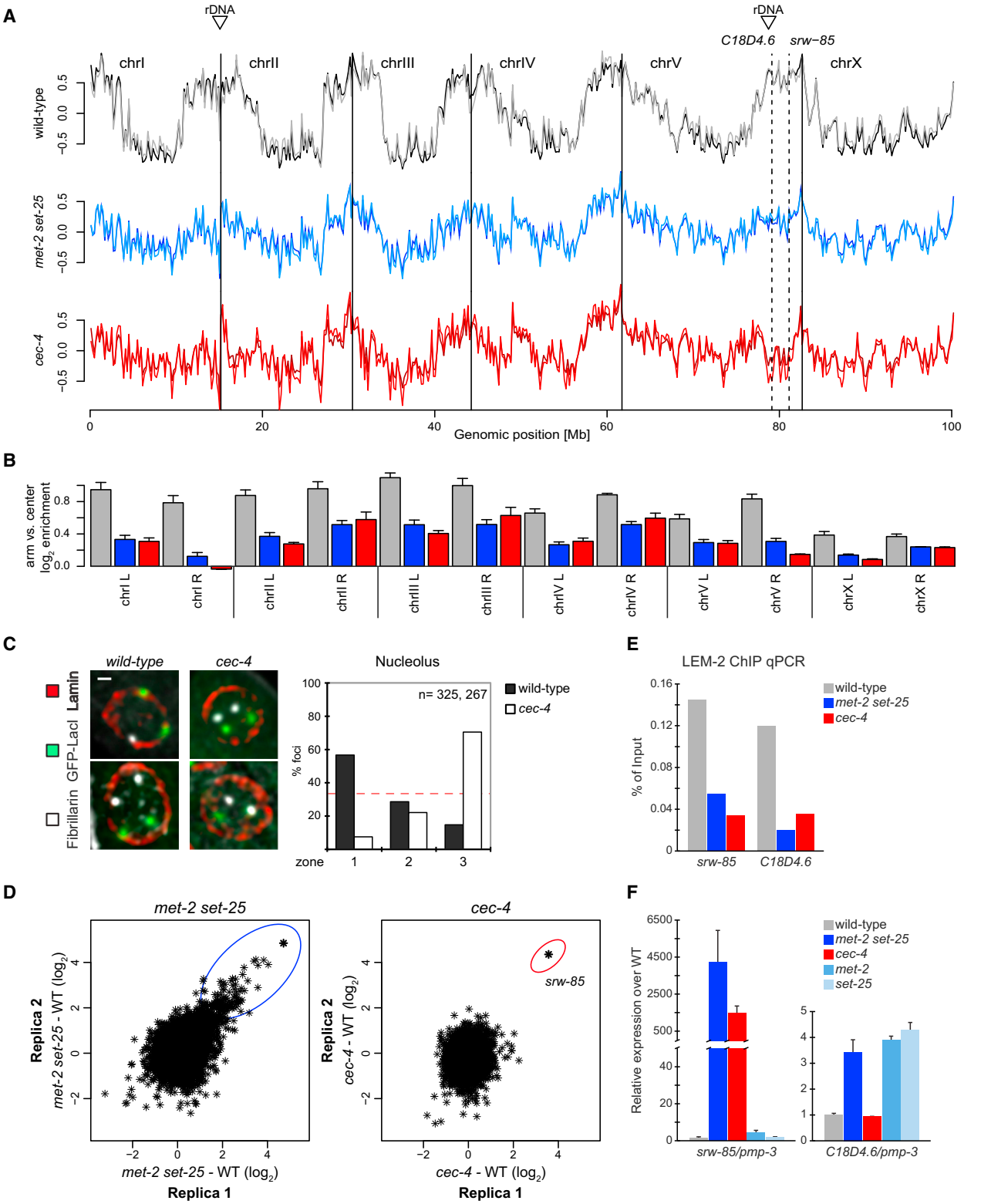

Figure 5. CEC-4 Influences Anchoring of Endogenous Chromatin and Nucleoli, but Not Silencing

(A) LEM-2 ChIP-seq profiles over chromosomes are shown for two independent replicas of early embryos of WT (gray/dark gray), *met-2 set-25* (blue/light blue), and *cec-4* (red/light red) mutants. Dashed line shows *srw-85* and *C18D4.6* genes, and triangles show rDNA clusters.

(legend continued on next page)

in vivo. Ablation of CEC-4 delocalizes heterochromatin, but does not necessarily lead to its derepression, whereas loss of histone H3K9 methylation compromises both. Other H3K9me-ligands (HP1 homologs HPL-1 and HPL-2, or LIN-61) contribute to transcriptional repression by binding H3K9me2 or me3, but do not mediate perinuclear anchoring. This bifurcation in function of a single methylated lysine in a histone tail, through divergent sets of methyl-lysine readers, provides a paradigm for how epigenetic states can coordinate distinct activities. In this case, chromatin can be anchored without silencing and silenced without anchoring, even though the two functions are correlated through H3K9 methylation. H3K9me1/me2 is sufficient for tethering through CEC-4, while H3K9me3 is needed for gene repression mediated by other H3K9me-readers (Figure 7). It remains to be seen if CEC-4 and other H3K9me readers interact.

CEC-4 Contributes to the Robustness of Ectopically Induced Differentiation

This finding gave us the opportunity to examine what happens during development when heterochromatin anchorage is compromised, without loss of H3K9 methylation or the transcriptional repression it mediates. Although *cec-4* mutant embryos yielded normal adult worms when development proceeded unperturbed, we were able to demonstrate a function for heterochromatin anchoring in early development by inducing muscle differentiation with ectopic expression of MyoD (HLH-1). Unlike the WT strain, a significant fraction of *cec-4* deficient embryos (about 25%) did not maintain the muscle fate provoked by HLH-1 induction (Figure 6) and continued to develop. In contrast, the induction of muscle cell fate and repression of alternative programs of differentiation occurred in 100% of the WT bean-staged embryos. The failure of the mutant to sustain an HLH-1-induced muscle program could either mean that CEC-4 actively supports muscle-specific gene expression, or else that it helps repress other tissue-specific programs. Given that muscle markers were expressed in heat-shocked *cec*-4 mutant embryos and that muscles develop normally in the mutant without HS, we favor the latter hypothesis: upon loss of CEC-4-mediated heterochromatin sequestration, non-muscle programs may not be properly repressed during ectopic muscle induction. This is consistent with earlier studies that showed a clear spatial segregation of active and inactive tissue-specific genes in differentiated cells of *C. elegans* larvae (Meister et al., 2010).

Because *cec-4* ablation per se seems to have a very limited effect on normal transcription patterns, we propose that CEC-4-mediated tethering does not control gene repression directly, but instead influences events that prepare genes for tissue-restricted patterns. These events might be the remodeling of epigenetic states (e.g., through histone deacetylases that bind the nuclear envelope [Zullo et al., 2012]), the sequestration of promoters away from their regulators, or the timing of replication of tissue-specific genes (Hiratani et al., 2008). These changes may not directly repress transcription, but rather change the compaction state of chromatin as a prerequisite for stage-specific repression. Indeed, the INM-released arrays in *cec-4* mutants are less compact (Figure 1), although we did not detect less histone H3K9 methylation by genome-wide ChIP (data not shown).

ESC differentiation studies have shown that the timing of replication of genes, and their reassembly into chromatin following replication, are compromised by spatial misorganization (reviewed in Hiratani et al., 2009). Moreover, it has been suggested that altered replication timing precedes commitment to differentiation-related expression patterns (Hiratani et al., 2008). Thus, we propose that CEC-4-mediated chromatin positioning and compaction may contribute to a replication timing program, which in turn reinforces appropriate gene repression. We expect that the compromised commitment of *cec-4* mutant is not restricted to muscle differentiation, but rather is a general mechanism that becomes important when normal development is perturbed. Whereas the ectopic HLH-1 induction is definitely a strong perturbation, less dramatic perturbations during development may rely on spatial sequestration to ensure proper patterns of tissue-specific gene expression.

Extending Nuclear Anchoring Mechanisms to Other Organisms

Although CEC-4 is the first CD protein reported to form a ring at the nuclear perimeter autonomously, CEC-4's anchoring function becomes either redundant or replaced by other mechanisms in L1 larvae, the stage at which most cells reached terminal differentiation. We note that heterochromatin can be anchored in differentiated tissues without H3K9 methylation, and without HPL-1, HPL-2, or LIN-61 (Studencka et al., 2012b; Towbin et al., 2012). Another CD protein, CEC-3, had no impact on embryonic array distribution in our screen, although it appears to restrain the expression of a neuronal specific transcription factor in larvae (Greer et al., 2014; Zheng et al., 2013). Thus, four H3K9me binders—HPL-1, HPL-2, LIN-61 and CEC-3—contribute to transcriptional silencing during development, while CEC-4 specifically sequesters H3K9me-containing chromatin in embryos. CEC-4 may also contribute to heterochromatin anchoring in some differentiated worm tissues, albeit in a redundant manner (data not shown).

(B) LEM-2 ChIP enrichment of arms (left or right) compared with corresponding center plotted for each genotype. Error bars = SEM.
(C) Representative merged color, single plane nuclei are shown for WT and *cec-4* mutant stained for anti-fibrillarin, lamin, and *gwIs4* array (anti-GFP), Scale bar, 2 μm. Zoning assay of nucleolar foci in 50–250 cell stage embryos, n = foci scored; pair-wise comparison p value < 0.001, χ^2 test.
(D) Relative gene expression profiles as scatter plots of *met-2 set*-25 and cec-*4* mutants versus WT early embryo extracts. Genes significantly changed are circled, bold star = *srw-85*.
(E) LEM-2 ChIP qPCR for *srw-85* and *C18D4.6* genes. ChIP values as a percentage of respective input DNA.
(F) Gene expression levels of indicated genotypes by qRT-PCR, normalized to *pmp-3* gene and shown relative to WT expression. Error bars = SEM of 3 biological replicas.
See also Figure S5.

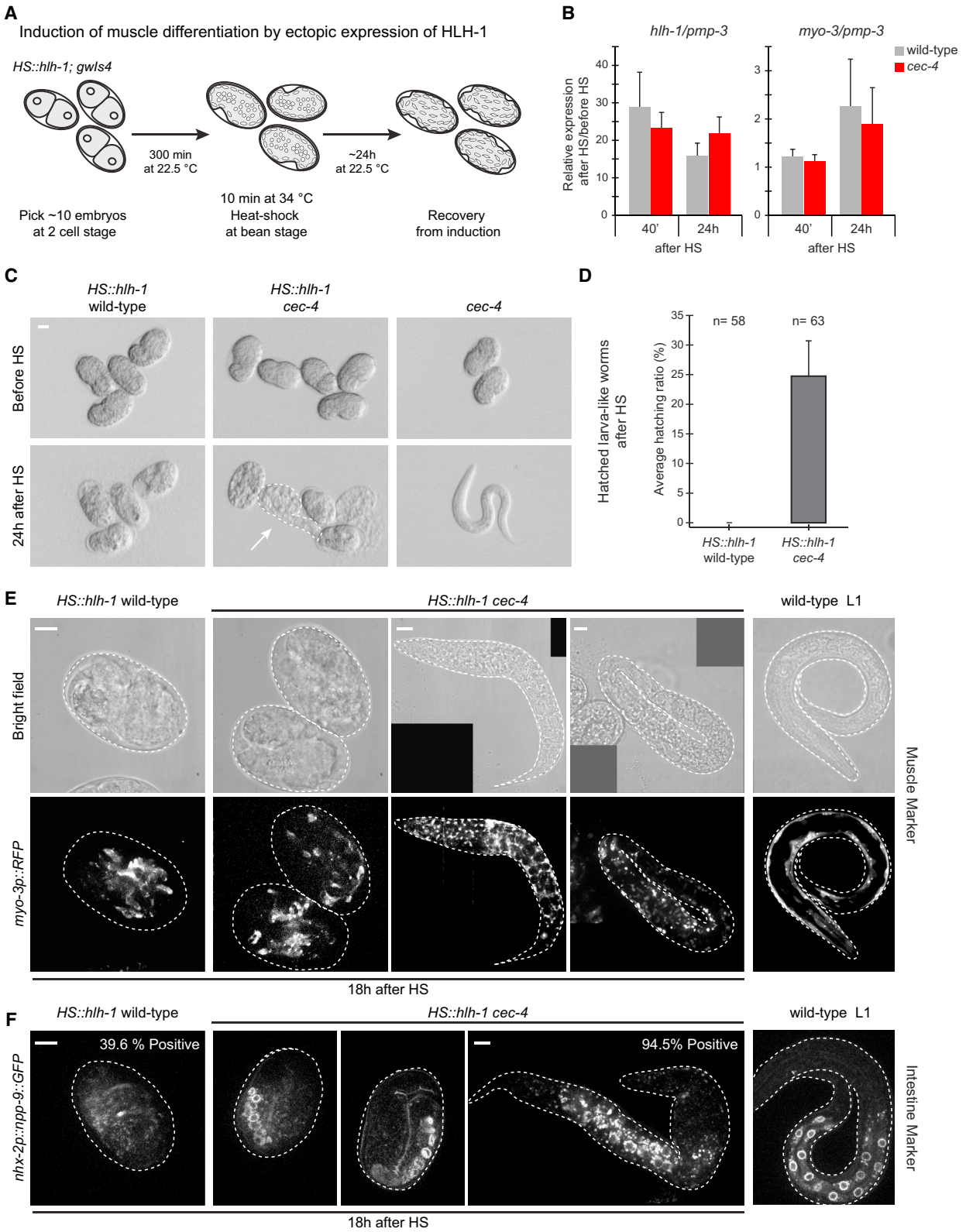

Figure 6. Lack of CEC-4 Impairs the Commitment of Embryos to a Forced Muscle Differentiation

(A) Experimental flow for forced muscle differentiation by HS induction of the master regulator HLH-1. See main text and Supplemental Experimental Procedures.

(legend continued on next page)

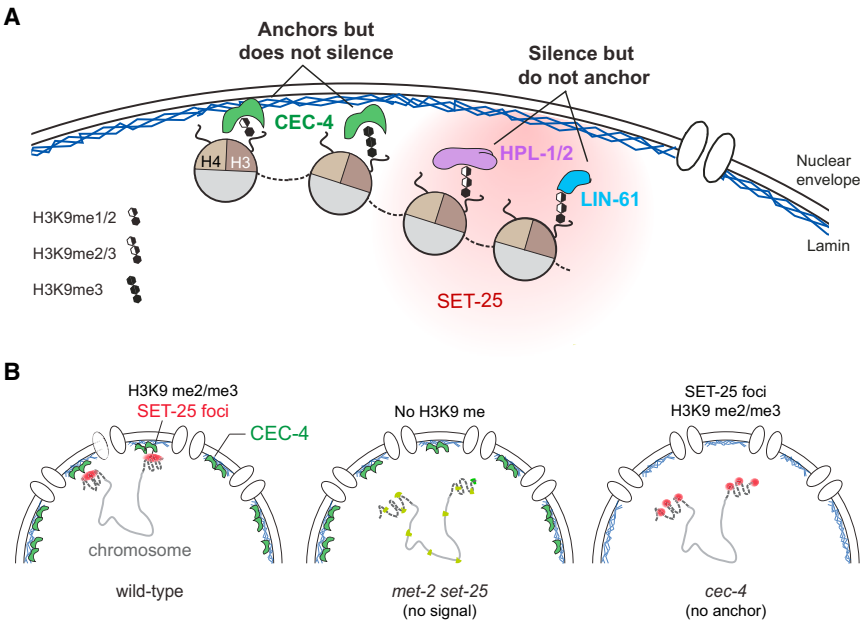

Figure 7. Different H3K9 me1, me2, and/or me3 Ligands Mediate Anchoring and Transcriptional Repression

(A) Model showing the split function of H3K9me for anchoring and repression thanks to different ligands.

(B) Summary of chromosome organization in early embryos in indicated genotypes. In WT embryos H3K9 methylation-enriched chromosome arms (dash lines) bind CEC-4 at the INM and are enriched for SET-25 (red foci). Lack of H3K9 methylation (*met-2 set-25* mutant) releases heterochromatin in embryos and derepresses genes (light green spots). Loss of CEC-4 compromises chromatin position, but does not induce gene expression.

We have not identified a direct homolog of CEC-4 in non-nematode species, and we suspect that this protein's two functions, INM-association and specific H3K9me-recognition, may be embodied in two separate polypeptides in mammals. As mentioned, an example of such split function may be the mammalian nuclear membrane-spanning protein PPR14, which can bind HP1. The interpretation that PPR14 anchors heterochromatin through this ligand is complicated, however, by the pleiotropic effects its loss has on nuclear shape (Poleshko et al., 2013). Similarly, the mammalian LBR may bind HP1 and carries a Tudor domain with a preference for H4K20me2 in vitro (Hirano et al., 2012; Ye and Worman, 1996). Whereas there is no compelling evidence that either H4K20me2 or HP1 mediate perinuclear anchoring in early development, LBR itself is implicated in the spatial organization of the genome in differentiated mammalian cells, particularly in cells that do not express Lamin A/C (Clowney et al., 2012; Solovei et al., 2013). Unfortunately, indirect effects again complicate the interpretation of LBR ablation, since this transmembrane protein has sterol reductase activity that regulates cholesterol metabolism and maintains appropriate spacing between inner and outer nuclear membranes (Holmer et al., 1998). Thus, both indirect effects and redundancy among anchors have made it difficult to characterize chromatin-tethering pathways in mammalian cells. Nonetheless, it is possible that these INM proteins function through chromatin binding proteins that resemble CEC-4. Separation of function mutations that uniquely compromise chromatin positioning will be needed to define these pathways unequivocally.

In other species, repressive epigenetic marks other than H3K9 methylation may contribute to the spatial sequestration of repressed chromatin. In mouse 3T3 embryonic fibroblasts (MEFs), the Polycomb mark H3K27me3 was reported to contribute to perinuclear positioning at the edges of LADs (Harr et al., 2015). In worms, the loss of Polycomb components MES-3 and MES-6 led to derepression of our heterochromatic reporter in embryos (Towbin et al., 2012), but did not trigger release from the nuclear periphery. Moreover, in most species, the H3K27me3-positive foci found in differentiating cells are not perinuclear (Eberhart et al., 2013). This, however, does not preclude the possibility that combinatorial epigenetic signatures target chromatin to the INM.

The relative simplicity of the *C. elegans* system and the conserved nature of its epigenetic and developmental programs has allowed us to dissect nuclear organization with a genetic approach. Given the conserved role H3K9me has in chromatin positioning, it is likely that factors with analogous functions as CEC-4 exist elsewhere. Functional screens in compromised backgrounds will be able to shed light on relevant anchors in differentiated cells. Disruption of specific anchors in differentiated tissues will extend our understanding of the function of heterochromatin sequestration.

(B) Quantitation of *hlh-1* and muscle specific *myo-3* expression by qRT-PCR in indicated genotypes, 40 min and 24 hr after HS relative to before HS; data normalized to *pmp-3* gene. Error bars = SEM of 3 biological replicas.

(C) Stereoscopic representative images of synchronized bean stage embryos before and 24 hr after HS. As control, *cec-4* null embryos lacking *HS::hlh-1* were treated similarly. Hatched larva-like worms highlighted with dashed white line and arrow. Scale bar, 20 μm.

(D) Average hatching ratio after HS according to genotype in bar plot. Error bars = SEM of six independent assays, n = total embryos tested.

(E) Muscle reporter pattern for indicated genotypes. Z-projections of bright field and fluorescent *myo-3p::RFP* (from *gwIs4*) imaging taken 18 hr after HS. Wild-type L1 imaged independently. Scale bars = 5 μm.

(F) Intestine reporter *nhx-2p::npp-9::GFP* pattern for indicated genotypes. Z-projections taken as in (E). n = 3, total number of embryos scored = 53 and 55 respectively. Scale bars,5 μm.

See also Figure S6.

EXPERIMENTAL PROCEDURES

RNAi Screen

RNAi was performed at 22.5°C by placing L1 worms on feeding plates as previously described (Timmons et al., 2001). For the list of genes used (Table S3) in the RNAi screen see Supplemental Experimental Procedures.

Microscopy

Microscopy was carried out on a spinning disc confocal microscope, using 2% agarose pads for live-microscopy or poly-lysine coated slides for fixed samples. Acquisition and analysis of array and nucleolus distribution, array spot volume, expression levels of GFP-LacI and CEC-4-mCh, and enrichment of CEC-4 over array are online, along with a description of super resolution-structured illumination microscopy (SR-SIM; Elyra S.1 [Carl Zeiss]).

AlphaScreen Direct Binding and In Vitro Assays

Purified recombinant His-tagged CEC-4 CD (200 nM) was screened for its binding to modified histone peptides with the ALTA Biosciences peptide array system (Alta Biosciences, UK) and the AlphaScreen assay. Details for protein purification, peptide pull down and ITC are in Supplemental Experimental Procedures.

LEM-2 ChIP-Seq and RNA-Seq

Early embryonic progeny was harvested after synchronization (60–65 hr depending on each strain) for WT, *met-2 set-25,* and *cec-4* mutant strains in two independent biological replicates. LEM-2 ChIP was performed as described (Ikegami et al., 2010). Total RNA was extracted by phenol/chloroform, further purified, and depleted for rRNA. Detailed information about library preparation and data analysis is described in Supplemental Experimental Procedures.

Heat-Shock Induced Muscle Differentiation

Two cell-stage embryos, of different genetic backgrounds containing the *HS::hlh-1* transgene, were allowed to develop until bean stage (300 min at 22.5°C). HS at 34°C for 10 min was performed either on 2% agarose pads or on liquid with a thermal cycler with in situ slide block. After recovery for 24 hr, evaluation of hatching larva-like worms was determined by stereomicroscopy, and reporter markers by spinning disc confocal microscopy. Details for qPCR of HS samples is described in Supplemental Experimental Procedures.

ACCESSION NUMBERS

The accession numbers for the ChIP-seq and RNA-seq data reported in this paper is NCBI Gene Expression Omnibus GEO: GSE74134.

SUPPLEMENTAL INFORMATION

Supplemental Information includes Supplemental Experimental Procedures, six figures, and seven tables and can be found with this article online at http://dx.doi.org/10.1016/j.cell.2015.10.066.

AUTHOR CONTRIBUTIONS

Conceptualization, A.G.-S., B.D.T., and S.M.G.; Methodology, A.G.-S., B.D.T., and D.S.C.; Validation, A.G.-S., V.K., D.S.C.; Formal Analysis, D.G., M.H.H; Investigation, A.G.-S., B.D.T., V.K., D.S.C., M.H.H, L.G., L.W., T.Y., X.W.; Resources, K.Z.; Writing – Review & Editing, A.G.-S., B.D.T., D.S.C., S.M.G.; Supervision, K.Z., S.M.G.; Funding Acquisition, S.G.M.

ACKNOWLEDGMENTS

Some strains were provided by the *Caenorhabditis* Genetics Center (CGC) of the NIH Office of Research Infrastructure Programs (P40 OD010440). We thank G-J. Hendriks, H. Grosshans, R. Thierry, P. Zeller, A. Peters, P. Hein, Y. Gruenbaum, and P. Askjaer for reagents and materials. We thank J. Lieb and K. Ikegami for training A.G.-S. in LEM-2 ChIP. We thank the FMI Worm, Genomics, Protein Structure, Protein Analysis, and Microscopy facilities for valuable advice and support. A.G.-S. was supported by FP7 Marie Curie Network Nucleosome 4D and the SNSF NCCR "Frontiers in Genetics." S.M.G. thanks the FMI and SNSF for support.

Received: July 1, 2015
Revised: October 7, 2015
Accepted: October 27, 2015
Published: November 19, 2015

REFERENCES

Barski, A., Cuddapah, S., Cui, K., Roh, T.-Y., Schones, D.E., Wang, Z., Wei, G., Chepelev, I., and Zhao, K. (2007). High-resolution profiling of histone methylations in the human genome. Cell *129*, 823–837.

Brachner, A., and Foisner, R. (2011). Evolvement of LEM proteins as chromatin tethers at the nuclear periphery. Biochem. Soc. Trans. *39*, 1735–1741.

Clowney, E.J., LeGros, M.A., Mosley, C.P., Clowney, F.G., Markenskoff-Papadimitriou, E.C., Myllys, M., Barnea, G., Larabell, C.A., and Lomvardas, S. (2012). Nuclear aggregation of olfactory receptor genes governs their monogenic expression. Cell *151*, 724–737.

Couteau, F., Guerry, F., Muller, F., and Palladino, F. (2002). A heterochromatin protein 1 homologue in Caenorhabditis elegans acts in germline and vulval development. EMBO Rep. *3*, 235–241.

Eberhart, A., Feodorova, Y., Song, C., Wanner, G., Kiseleva, E., Furukawa, T., Kimura, H., Schotta, G., Leonhardt, H., Joffe, B., and Solovei, I. (2013). Epigenetics of eu- and heterochromatin in inverted and conventional nuclei from mouse retina. Chromosome Res. *21*, 535–554.

Etchberger, J.F., Lorch, A., Sleumer, M.C., Zapf, R., Jones, S.J., Marra, M.A., Holt, R.A., Moerman, D.G., and Hobert, O. (2007). The molecular signature and cis-regulatory architecture of a C. elegans gustatory neuron. Genes Dev. *21*, 1653–1674.

Fischle, W., Wang, Y., and Allis, C.D. (2003a). Binary switches and modification cassettes in histone biology and beyond. Nature *425*, 475–479.

Fischle, W., Wang, Y., Jacobs, S.A., Kim, Y., Allis, C.D., and Khorasanizadeh, S. (2003b). Molecular basis for the discrimination of repressive methyl-lysine marks in histone H3 by Polycomb and HP1 chromodomains. Genes Dev. *17*, 1870–1881.

Fukushige, T., and Krause, M. (2005). The myogenic potency of HLH-1 reveals wide-spread developmental plasticity in early C. elegans embryos. Development *132*, 1795–1805.

Fussner, E., Ahmed, K., Dehghani, H., Strauss, M., and Bazett-Jones, D.P. (2010). Changes in chromatin fiber density as a marker for pluripotency. Cold Spring Harb. Symp. Quant. Biol. *75*, 245–249.

Gerstein, M.B., Lu, Z.J., Van Nostrand, E.L., Cheng, C., Arshinoff, B.I., Liu, T., Yip, K.Y., Robilotto, R., Rechtsteiner, A., Ikegami, K., et al.; modENCODE Consortium (2010). Integrative analysis of the Caenorhabditis elegans genome by the modENCODE project. Science *330*, 1775–1787.

González-Aguilera, C., Ikegami, K., Ayuso, C., de Luis, A., Íñiguez, M., Cabello, J., Lieb, J.D., and Askjaer, P. (2014). Genome-wide analysis links emerin to neuromuscular junction activity in Caenorhabditis elegans. Genome Biol. *15*, R21.

Greer, E.L., Beese-Sims, S.E., Brookes, E., Spadafora, R., Zhu, Y., Rothbart, S.B., Aristizábal-Corrales, D., Chen, S., Badeaux, A.I., Jin, Q., et al. (2014). A histone methylation network regulates transgenerational epigenetic memory in C. elegans. Cell Rep. *7*, 113–126.

Gudise, S., Figueroa, R.A., Lindberg, R., Larsson, V., and Hallberg, E. (2011). Samp1 is functionally associated with the LINC complex and A-type lamina networks. J. Cell Sci. *124*, 2077–2085.

Guelen, L., Pagie, L., Brasset, E., Meuleman, W., Faza, M.B., Talhout, W., Eussen, B.H., de Klein, A., Wessels, L., de Laat, W., and van Steensel, B. (2008). Domain organization of human chromosomes revealed by mapping of nuclear lamina interactions. Nature *453*, 948–951.

Harr, J.C., Luperchio, T.R., Wong, X., Cohen, E., Wheelan, S.J., and Reddy, K.L. (2015). Directed targeting of chromatin to the nuclear lamina is mediated by chromatin state and A-type lamins. J. Cell Biol. *208*, 33–52.

Hirano, Y., Hizume, K., Kimura, H., Takeyasu, K., Haraguchi, T., and Hiraoka, Y. (2012). Lamin B receptor recognizes specific modifications of histone H4 in heterochromatin formation. J. Biol. Chem. *287*, 42654–42663.

Hiratani, I., Ryba, T., Itoh, M., Yokochi, T., Schwaiger, M., Chang, C.W., Lyou, Y., Townes, T.M., Schübeler, D., and Gilbert, D.M. (2008). Global reorganization of replication domains during embryonic stem cell differentiation. PLoS Biol. *6*, e245.

Hiratani, I., Takebayashi, S., Lu, J., and Gilbert, D.M. (2009). Replication timing and transcriptional control: beyond cause and effect–part II. Curr. Opin. Genet. Dev. *19*, 142–149.

Holmer, L., Pezhman, A., and Worman, H.J. (1998). The human lamin B receptor/sterol reductase multigene family. Genomics *54*, 469–476.

Ikegami, K., Egelhofer, T.A., Strome, S., and Lieb, J.D. (2010). Caenorhabditis elegans chromosome arms are anchored to the nuclear membrane via discontinuous association with LEM-2. Genome Biol. *11*, R120.

Kind, J., Pagie, L., Ortabozkoyun, H., Boyle, S., de Vries, S.S., Janssen, H., Amendola, M., Nolen, L.D., Bickmore, W.A., and van Steensel, B. (2013). Single-cell dynamics of genome-nuclear lamina interactions. Cell *153*, 178–192.

Koester-Eiserfunke, N., and Fischle, W. (2011). H3K9me2/3 binding of the MBT domain protein LIN-61 is essential for Caenorhabditis elegans vulva development. PLoS Genet. *7*, e1002017.

Kubben, N., Adriaens, M., Meuleman, W., Voncken, J.W., van Steensel, B., and Misteli, T. (2012). Mapping of lamin A- and progerin-interacting genome regions. Chromosoma *121*, 447–464.

Mattout, A., Aaronson, Y., Sailaja, B.S., Raghu Ram, E.V., Harikumar, A., Mallm, J.P., Sim, K.H., Nissim-Rafinia, M., Supper, E., Singh, P.B., et al. (2015). Heterochromatin Protein 1β (HP1β) has distinct functions and distinct nuclear distribution in pluripotent versus differentiated cells. Genome Biol. *16*, 213.

Meister, P., Towbin, B.D., Pike, B.L., Ponti, A., and Gasser, S.M. (2010). The spatial dynamics of tissue-specific promoters during C. elegans development. Genes Dev. *24*, 766–782.

Meister, P., Mango, S.E., and Gasser, S.M. (2011). Locking the genome: nuclear organization and cell fate. Curr. Opin. Genet. Dev. *21*, 167–174.

Meuleman, W., Peric-Hupkes, D., Kind, J., Beaudry, J.B., Pagie, L., Kellis, M., Reinders, M., Wessels, L., and van Steensel, B. (2013). Constitutive nuclear lamina-genome interactions are highly conserved and associated with A/T-rich sequence. Genome Res. *23*, 270–280.

Minc, E., Allory, Y., Worman, H.J., Courvalin, J.C., and Buendia, B. (1999). Localization and phosphorylation of HP1 proteins during the cell cycle in mammalian cells. Chromosoma *108*, 220–234.

Nestorov, P., Tardat, M., and Peters, A.H. (2013). H3K9/HP1 and Polycomb: two key epigenetic silencing pathways for gene regulation and embryo development. Curr. Top. Dev. Biol. *104*, 243–291.

Nigg, E.A. (1992). Assembly and cell cycle dynamics of the nuclear lamina. Semin. Cell Biol. *3*, 245–253.

Padeken, J., and Heun, P. (2014). Nucleolus and nuclear periphery: velcro for heterochromatin. Curr. Opin. Cell Biol. *28*, 54–60.

Peric-Hupkes, D., Meuleman, W., Pagie, L., Bruggeman, S.W., Solovei, I., Brugman, W., Gräf, S., Flicek, P., Kerkhoven, R.M., van Lohuizen, M., et al. (2010). Molecular maps of the reorganization of genome-nuclear lamina interactions during differentiation. Mol. Cell *38*, 603–613.

Pickersgill, H., Kalverda, B., de Wit, E., Talhout, W., Fornerod, M., and van Steensel, B. (2006). Characterization of the Drosophila melanogaster genome at the nuclear lamina. Nat. Genet. *38*, 1005–1014.

Pinheiro, I., Margueron, R., Shukeir, N., Eisold, M., Fritzsch, C., Richter, F.M., Mittler, G., Genoud, C., Goyama, S., Kurokawa, M., et al. (2012). Prdm3 and Prdm16 are H3K9me1 methyltransferases required for mammalian heterochromatin integrity. Cell *150*, 948–960.

Poleshko, A., Mansfield, K.M., Burlingame, C.C., Andrake, M.D., Shah, N.R., and Katz, R.A. (2013). The human protein PRR14 tethers heterochromatin to the nuclear lamina during interphase and mitotic exit. Cell Rep. *5*, 292–301.

Solovei, I., Wang, A.S., Thanisch, K., Schmidt, C.S., Krebs, S., Zwerger, M., Cohen, T.V., Devys, D., Foisner, R., Peichl, L., et al. (2013). LBR and lamin A/C sequentially tether peripheral heterochromatin and inversely regulate differentiation. Cell *152*, 584–598.

Steffen, P.A., Fonseca, J.P., and Ringrose, L. (2012). Epigenetics meets mathematics: towards a quantitative understanding of chromatin biology. BioEssays *34*, 901–913.

Studencka, M., Konzer, A., Moneron, G., Wenzel, D., Opitz, L., Salinas-Riester, G., Bedet, C., Krüger, M., Hell, S.W., Wisniewski, J.R., et al. (2012a). Novel roles of Caenorhabditis elegans heterochromatin protein HP1 and linker histone in the regulation of innate immune gene expression. Mol. Cell. Biol. *32*, 251–265.

Studencka, M., Wesołowski, R., Opitz, L., Salinas-Riester, G., Wisniewski, J.R., and Jedrusik-Bode, M. (2012b). Transcriptional repression of Hox genes by C. elegans HP1/HPL and H1/HIS-24. PLoS Genet. *8*, e1002940.

Taddei, A., and Gasser, S.M. (2012). Structure and function in the budding yeast nucleus. Genetics *192*, 107–129.

Talamas, J.A., and Capelson, M. (2015). Nuclear envelope and genome interactions in cell fate. Front. Genet. *6*, 95.

Taouji, S., Dahan, S., Bossé, R., and Chevet, E. (2009). Current Screens Based on the AlphaScreen Technology for Deciphering Cell Signalling Pathways. Curr. Genomics *10*, 93–101.

Taverna, S.D., Li, H., Ruthenburg, A.J., Allis, C.D., and Patel, D.J. (2007). How chromatin-binding modules interpret histone modifications: lessons from professional pocket pickers. Nat. Struct. Mol. Biol. *14*, 1025–1040.

Timmons, L., Court, D.L., and Fire, A. (2001). Ingestion of bacterially expressed dsRNAs can produce specific and potent genetic interference in Caenorhabditis elegans. Gene *263*, 103–112.

Towbin, B.D., Meister, P., Pike, B.L., and Gasser, S.M. (2010). Repetitive transgenes in C. elegans accumulate heterochromatic marks and are sequestered at the nuclear envelope in a copy-number- and lamin-dependent manner. Cold Spring Harb. Symp. Quant. Biol. *75*, 555–565.

Towbin, B.D., González-Aguilera, C., Sack, R., Gaidatzis, D., Kalck, V., Meister, P., Askjaer, P., and Gasser, S.M. (2012). Step-wise methylation of histone H3K9 positions heterochromatin at the nuclear periphery. Cell *150*, 934–947.

Unnikrishnan, A., Gafken, P.R., and Tsukiyama, T. (2010). Dynamic changes in histone acetylation regulate origins of DNA replication. Nat. Struct. Mol. Biol. *17*, 430–437.

Wilson, K.L., and Foisner, R. (2010). Lamin-binding Proteins. Cold Spring Harb. Perspect. Biol. *2*, a000554.

Ye, Q., and Worman, H.J. (1996). Interaction between an integral protein of the nuclear envelope inner membrane and human chromodomain proteins homologous to *Drosophila* HP1. J. Biol. Chem. *271*, 14653–14656.

Zheng, C., Karimzadegan, S., Chiang, V., and Chalfie, M. (2013). Histone methylation restrains the expression of subtype-specific genes during terminal neuronal differentiation in Caenorhabditis elegans. PLoS Genet. *9*, e1004017.

Zullo, J.M., Demarco, I.A., Piqué-Regi, R., Gaffney, D.J., Epstein, C.B., Spooner, C.J., Luperchio, T.R., Bernstein, B.E., Pritchard, J.K., Reddy, K.L., and Singh, H. (2012). DNA sequence-dependent compartmentalization and silencing of chromatin at the nuclear lamina. Cell *149*, 1474–1487.